J Mater Sci (2007) 42:1388–1392
DOI 10.1007/s10853-006-1427-3

LETTER

A peak in the hydration reaction at the end of the cement induction period

J. M. Makar · G. W. Chan · K. Y. Esseghaier

Received: 14 July 2006 / Accepted: 11 December 2006 / Published online: 23 January 2007

Although the hydration of ordinary Portland cement (OPC) and its main constituent, tricalcium silicate ($3CaO{\cdot}SiO_2$ or C_3S), have been studied for many decades [1], some aspects of the hydration process remain poorly understood. In particular, there is little consensus on the mechanisms related to the dormant or induction period [2, 3]. The induction period is a time of minimal hydration activity between the initial hydration reactions upon wetting and the later primary tricalcium silicate reaction with water to form calcium silicate hydrate and calcium hydroxide. This letter examines the mechanisms responsible for a peak in hydration activity at the end of the induction period. Although occasionally seen in the literature [4], this peak appears absent in most reported measurements and has therefore remained unexplained.

The hydration reactions were studied through conduction calorimetry, a standard method of measuring the heat produced during cement hydration and other processes [5–9]. Here, a new approach to the analysis of conduction calorimetry data through the use of derivatives was used. The presence of individual reactions can be more easily identified and the effects of changes in reaction conditions more easily traced using derivative analysis than by using standard conduction calorimetry alone. Similar advantages have been identified in the use of derivative differential thermal analysis [10], while derivative methods are also used in other forms of thermal analysis.

Both pure C_3S (surface area 0.32 m^2/g) and OPC samples were hydrated in a Thermometric Tam Air Isothermal Calorimeter (model 3114) using Accusolv (Anachemia, Inc.) water with a maximum impurity level of 1 ppm at a water/cement (w/c) ratio of 0.5 by mass. All measurements were conducted at a constant temperature of 24 °C. Most measurements were made at 1 min intervals, with one second intervals used for additional tests to confirm the primary results. All data were recorded using a computer based data acquisition system with a typical uncertainty of ±0.002 mW/g. While the C_3S and OPC results reported here are each from single commercial sources, similar results were observed for all cements that have been examined (seven C_3S and four OPC to date). The C_3S used in the initial work was also ground to produce samples with five different surface areas (determined by BET surface measurement), which were hydrated in the conduction calorimeter at the same w/c ratio.

The high signal to noise ratio of the recorded data allowed it to be smoothed (Sigmaplot 9.0, Systat Software, Inc.) to reduce the remaining background noise and allow derivatives to be taken. The smoothing was done using a Gaussian weighting function ($e^{-u\wedge 2}$, where u is the normalized distance of the data used in the smoothing), typically with a third order polynomial regression. Considerable care was taken to ensure that the smoothing process did not affect the underlying shape of the hydration curve. First and second order derivatives of the heat

J. M. Makar (✉) · G. W. Chan · K. Y. Esseghaier
Institute for Research in Construction, National Research Council Canada, 1200 Montreal Road, Ottawa, ON Canada K1A 0R6
e-mail: jon.makar@nrc-cnrc.gc.ca

flow data with respect to time were then calculated using a standard numerical approach [11]. No additional information was gained from the second order derivatives.

Samples of as-delivered C_3S at the same w/c ratio were also hydrated for times ranging from a half hour to 4 h under ambient conditions for additional study. The hydration was stopped by washing in excess isopropanol and the samples dried for 24 h in a vacuum oven. This procedure may change the morphology of later hydration products, but has been used successfully to prepare early stage hydration samples for transmission electron microscopy [12]. The samples were then analyzed using differential scanning calorimetry (DSC) (TA Instruments SDT Q-600) under nitrogen gas and cold field emission scanning electron microscopy (CFESEM, Hitachi S-4800). The CFESEM imaging was undertaken at an emission current of 4 μA and an accelerating voltage of 1 kV on uncoated samples, allowing for greater resolution of details of the surface than has typically been reported in the cement literature.

Figure 1a, b show typical conduction calorimetry data and the corresponding time derivatives for tricalcium silicate and OPC respectively, with Fig. 1c, d showing the corresponding induction period behaviour. The numbers on the graphs indicate the various reaction peaks in the heat flow plots and their corresponding maximum time derivatives. Peaks 1–3 are common to both materials, while peaks 4 and 5 only occur in OPC and have been associated with reactions by constituents other than C_3S [13]. The initial reactions upon wetting (peak 1, both figures) and the main tricalcium silicate reaction (peak 3, both figures) are well known [1]. Although peak 1 occurs in both materials, in OPC it is predominated by the initial tricalcium aluminate ($3CaO{\cdot}Al_2O_3$) hydration reactions. As very early data was subject to fluctuations produced as the apparatus establishes thermal equilibrium, only the final stages of peak 1 are shown.

Peak 2, the focus of this letter, is not well studied. Its presence in both examined materials indicates an origin in a C_3S reaction, while its temporal position suggests an association with the events that cause the end of induction period. Peak 2 may be difficult to discern in commercial cements without high resolution conduction calorimetry measurements. However, grinding cement samples to increase their surface area greatly enhances the heat produced during peak 2, producing values that can readily be measured (Fig. 2). In addition, the point marked I in Fig. 1c became identifiable as a separate hydration peak. The derivatives in Fig. 1c show the shape expected from exothermic cement hydration reactions, with an initial maxima followed by a minima.

The DSC results during the calcium hydroxide decomposition of the as-delivered C_3S paste (Fig. 3a) showed that a change in the rate of growth of the

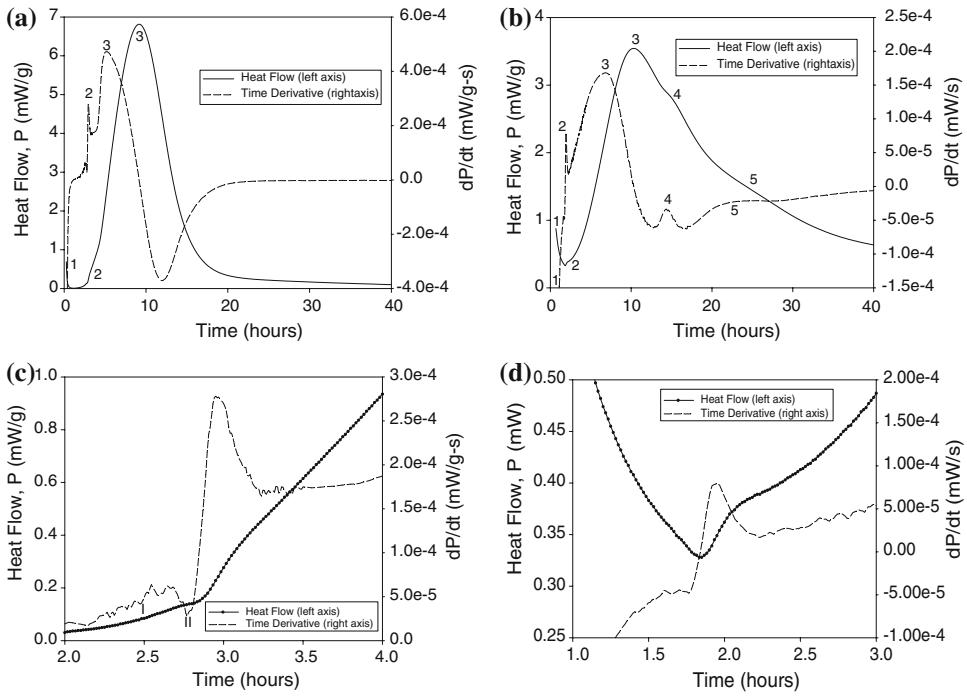

Fig. 1 Measured conduction calorimetry data (solid and dotted solid lines) and time derivatives (dashed lines) for tricalcium silicate and OPC. (**a**) Tricalcium silicate hydration. (**b**) OPC hydration. (**c**) and (**d**) Close-ups at the time of peak 2 of a and b respectively, with the dots indicating individual experimental data points

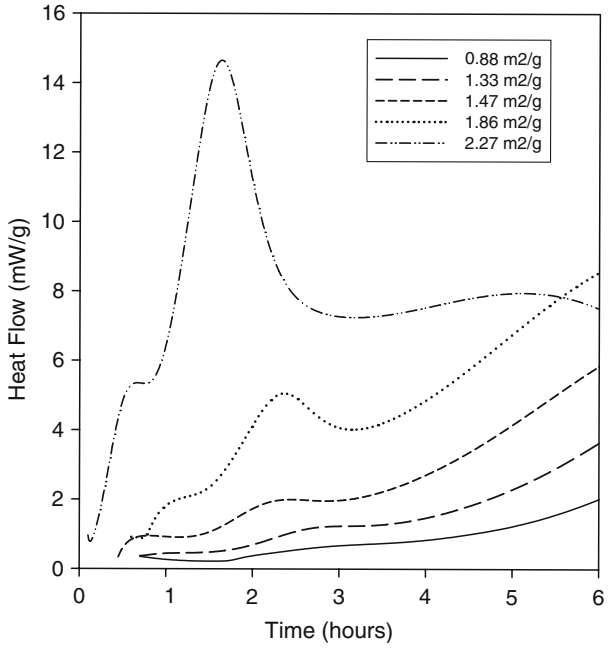

Fig. 2 Effect of C_3S grain surface area on the size of peak 2

calcium hydroxide in the samples occurs at the onset of peak 2 (Fig. 3b, c), with slower growth rates occurring immediately after the peak than before it. Moreover, the CFESEM examination showed distinct morphological changes associated with the peak 2 reaction. Unhydrated grains showed no reaction products (Fig. 4a). While individual cement grains varied due to local reaction conditions, almost all C_3S grains observed at 2.5 h of hydration had smooth surfaces with minimal porosity (arrows, Fig. 4b) and hydration products. Immediately before peak 2, shallow, 10–30 nm wide pores and increased hydration products were more widespread (Fig. 4c), but many regions remained pore free. During the peak 2 reaction, the pores deepened and became more common, while the hydration products increased in size and grew away from the surface (Fig. 4d). Further increases in size of the pores and the hydration products were seen after peak 2 (Fig. 4e). The same pattern of behaviour was observed in both the finely ground C_3S and the OPC samples. Similar, although much larger, porosity has been reported previously during the hydration of C_3S pellets [14], while the calcium silicate hydrate structures appear to correspond to those observed by transmission electron microscopy [12].

The conduction calorimetry results in Fig. 2, the change in the rate of formation of calcium hydroxide at peak 2 (Fig. 3) and the CFESEM images all suggest that peak 2 is related to behaviour at the surface of the cement grains. Previous work [14, 15] has suggested that a protective layer forms on the surface of the C_3S during peak 1, which inhibits further hydration reactions. For the C_3S used here, hydration products formed in small quantities on the grain surface towards the end of the induction period, producing a slight increase in heat flow

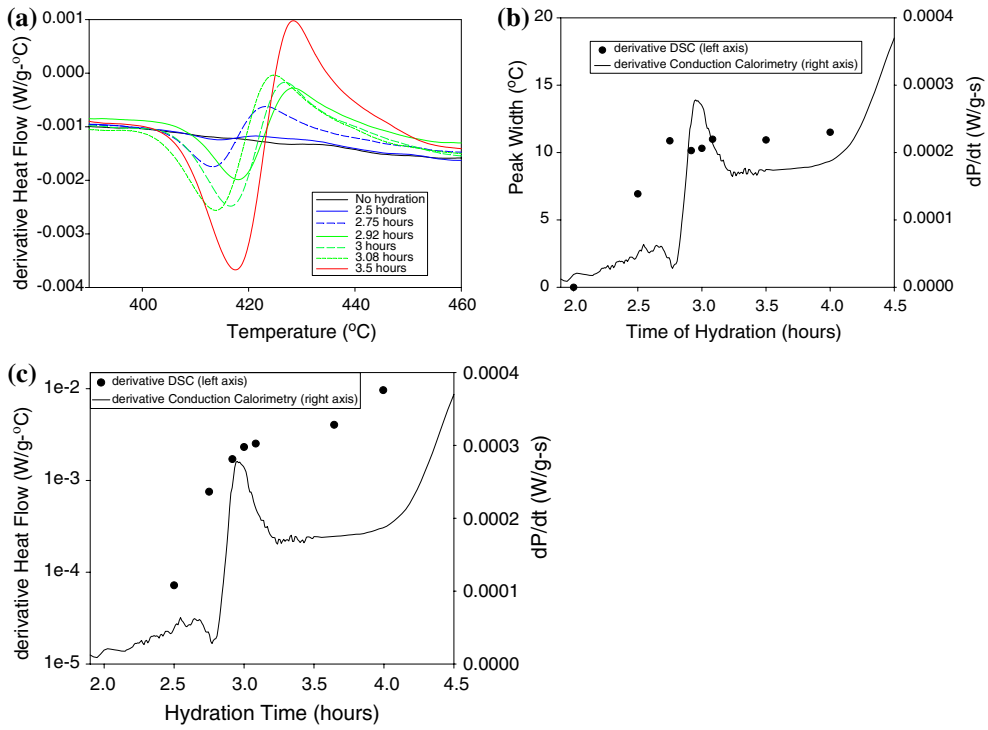

Fig. 3 Derivative differential scanning calorimetry (DSC) results for the tricalcium silicate in Fig. 1. (**a**) Response during decomposition of calcium hydroxide. Blue lines are before the onset of peak 2, green during peak 2 and red after peak 2. Results for 0.5, 1, 2 and 4 h are not shown for clarity. (**b**) Peak to peak width for calcium hydroxide decomposition curves, measured as the temperature difference between the maximum and minima derivative DSC values in a. The measurements are ±0.5 °C. (**c**) Peak to peak value for calcium hydroxide decomposition, measured as the difference in derivative DSC values between the maximum and minima points for each curve in a. Peak to peak measurements are ±2e–5 °C

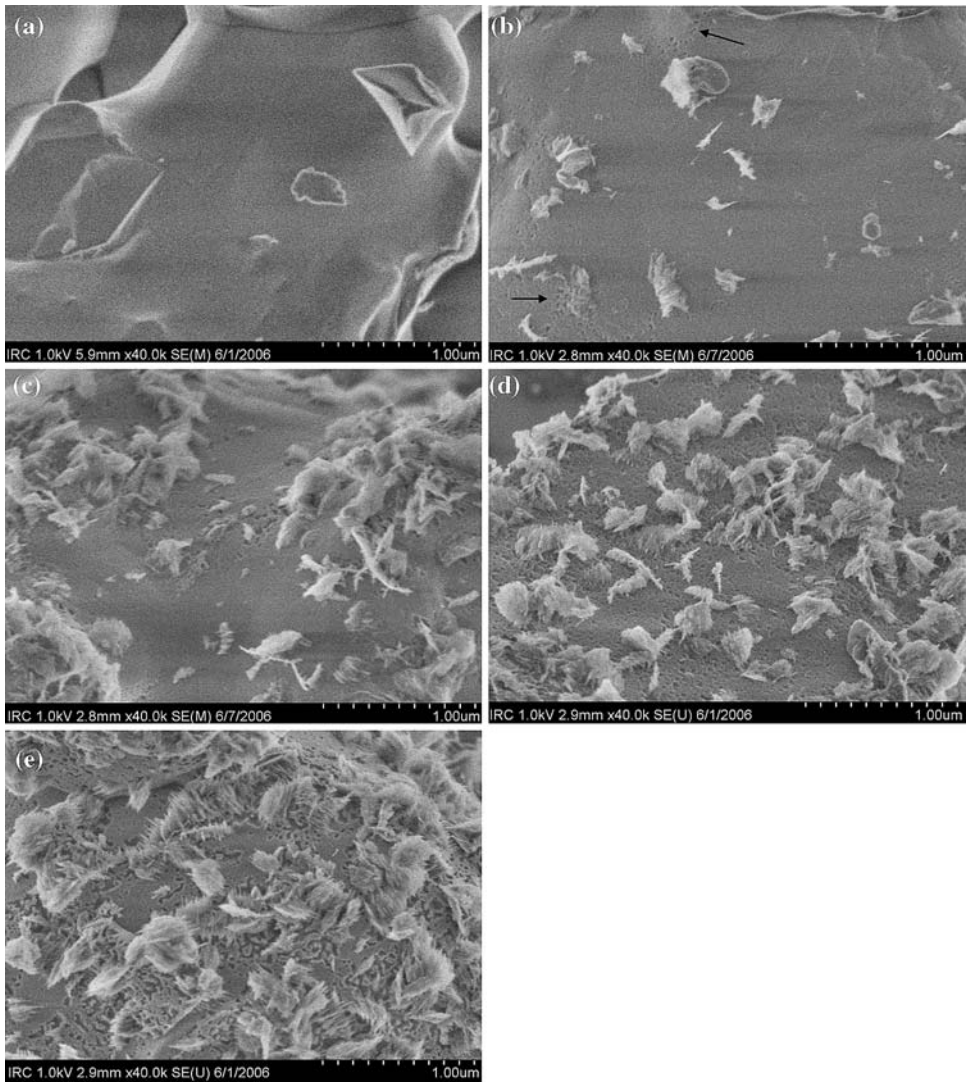

Fig 4 Cold field emission SEM images of unhydrated tricalcium silicate (**a**) and tricalcium silicate hydrated for 2.5 (**b**), 2.75 (**c**), 2.92 (**d**) and 4 (**e**) hours

(Fig. 1c, Point I). The rate of change in the heat flow then dropped (Point II), suggesting a reduced availability of reaction precursors. This effect was increased in the high surface area examples in Fig. 2. The protective layer then appears to have been penetrated and pores formed in the surface of the grain. The renewed availability of reaction precursors allowed the grain surface to be covered with hydration products, producing peak 2 and the rapid increase in calcium hydroxide formation in Fig. 3. Peak 2 increased with increasing surface area as more sites were available for pores and surface hydration products to form. Peak 2 then ended as the available sites for pore formation and hydration product nucleation on the surface of the grain were consumed. After this point, nucleation and growth processes on the existing hydration products dominated the hydration reaction, producing peak 3 and a slower rate of increase in calcium hydroxide formation. It is worth noting that while all the hydration reactions are exothermic, the pore formation process might possibly be endothermic in nature, as its thermal behaviour is masked by the simultaneous hydration product formation.

As peak 2 represents a surface effect, increasing grain size or the contamination of the surface of unhydrated OPC or C_3S through carbonation or partial hydration would be expected to reduce its extent. Further work is needed to understand the implications of the process that creates peak 2 on the operation of chemical admixtures such as superplasticizers, which are believed to function at the surface of hydrating cement grains [16]. Work is also needed to incorporate the existence of peak 2 into the existing models [2, 3] for the early stages of cement hydration, which do not include the processes described here.

Acknowledgements J.J. Beaudoin and V.S. Ramachandran provided useful comments in the writing of this paper. K. Trischuk provided the BET surface measurements. This research was funded by the National Research Council Canada.

References

1. Neville AM (1995) In: Properties of concrete, 4th edn. Pearson Education Limited, p 13
2. Taylor HFW (1997) In: Cement chemistry, 2nd edn. Thomas Telford, London, p 153
3. Taylor HFW et al (1984) Materiaux et Constructions 17:457
4. Longuet P (1969) In: Proceedings of the fifth international symposium on the chemistry of cement (Tokyo, Oct 7–11, 1968), Part II, vol II, 30
5. Ramachandran VS et al (2003) In: Handbook of thermal analysis of construction materials. Noyes Publications, Norwich, New York, p 26
6. Smith AL, Shirazi HM, Smith FC (2005) Catalysis Lett 104:199
7. Delgado-Sanchez JM et al (2005) J Phys (D) Cond Mat 17:2645
8. Bunyan P, Baker C, Turner N (2003) Thermo Acta 401:9
9. Maskow T, Babel W, (2003) J Biotechnol 101:267
10. Ramachandran VS (1969) In: Applications of differential thermal analysis in cement chemistry. Chemical Publishing Company, New York, p 48
11. Ralston A, Rabinowitz P (2001) In: A first course in numerical analysis. Dover Publications, Mineola, New York, p 93
12. Henderson E, Bailey JE (1993) J Mater Sci 28:3681
13. Pratt PL, Ghose A (1983) Phil Trans R Soc Lond A 310:93
14. Ménétrier D et al (1979) Cem Conc Res 9:473
15. Clark SM, Morrison GR, Shi WD (1999) Cem Conc Res 29:1099
16. Rixom R, Mailvaganam N (1999) In: Chemical admixtures for concrete, 3rd edn. E. & F.N. Spon, London, p 300